Analysis of fluctuations in ultra-small semiconductor devices

P. Andrei and I. D. Mayergoyz
ECE Department, University of Maryland
College Park, MD 20742
pandrei@eng.umd.edu

Abstract— **A technique for the analysis of fluctuations in ultra small semiconductor devices is presented. This technique is applied to the computation fluctuations of threshold voltages and terminal characteristics of MOSFET devices due to the random doping fluctuations and oxide roughness. It is based on the linearization of transport equations with respect to the fluctuating quantities. This approach completely avoids computations for many device realizations and, therefore, it is computationally much more efficient than Monte-Carlo techniques.**

Keywords-fluctuations; quantum effects; MOSFET; density gradient; simulations.

I. INTRODUCTION

The precision of analog and mixed signal electronic circuits depends in general on the accurate matching of electrical parameters of their components. Unfortunately, due to the random nature of ion implantation and diffusion processes and to the fluctuations of geometrical characteristics (oxide thickness, length, width, etc.), the electrical parameters of devices fluctuate around their nominal values [1]-[3]. Random doping and geometrical fluctuations are especially pronounced in small devices where spatial scales of these fluctuations are more or less comparable with device dimensions. They lead to appreciable fluctuations of threshold voltages [4], [5], small signal parameters [6], [7], and subthreshold characteristics [8] of semiconductor devices. For this reason, an accurate statistical analysis of random dopant-induced effects is very important for the further progress in semiconductor technology in general and mixed signal electronics in particular.

The existing approaches to the analysis of fluctuations in semiconductor devices are based on generating numerous realizations of devices and solving the transport equations for each of such realization (Monte-Carlo methods). In this way, statistics of different parameters of interest are accumulated and then used for the evaluation of variances of those parameters. These methods are computationally very expensive since the same device-level simulations have to be performed many times. A new method that overcomes these difficulties has been recently developed for the computation of random doping induced fluctuations of threshold voltage, drain current, and small signal parameters of MOSFET devices [4], [5], within the framework of classical drift-diffusion model. This method is based on the linearization of transport equations with respect to the fluctuating quantities and it is computationally much more efficient than the existing purely statistical methods. In addition, it provides information about the sensitivity of threshold voltages to the fluctuations of doping concentration and oxide thickness at different locations and, therefore, it is instrumental in the design of fluctuation-resistant structures. In this paper, we extend this technique to the analysis of threshold voltage (V_T) fluctuations of MOSFET devices induced by the random doping and random oxide roughness, and we take into account quantum mechanical effects within the framework of density gradient (DG) model. It should be noted that a similar approach can be used for the computation of fluctuations induced by other random parameters like the channel length and interface charge density.

Throughout this work, the electron and hole transport in the semiconductor is described by the density gradient (DG) model [9]. By considering the steady state case and by neglecting recombination, the DG model can be summarized by the following system of nonlinear, second order partial differential equations:

$$\nabla\cdot(\varepsilon\nabla\varphi)+q\left(p-n+N_D^+-N_A^-\right)=0, \tag{1}$$

$$\frac{2\nabla\cdot\left(b_n\nabla\sqrt{n}\right)}{\sqrt{n}}+\varphi-\phi_n-\frac{kT}{q}\ln\frac{n}{n_i}=0, \tag{2}$$

$$\frac{2\nabla\cdot\left(b_p\nabla\sqrt{p}\right)}{\sqrt{p}}-\varphi+\phi_p+\frac{kT}{q}\ln\frac{n_i}{p}=0, \tag{3}$$

$$\nabla\cdot\left(\mu_n n\nabla\phi_n\right)=0,\ \ \nabla\cdot\left(\mu_p p\nabla\phi_p\right)=0, \tag{4}$$

where ϕ_n and ϕ_p are the electron and hole quasi-Fermi potentials, respectively,

$$b_n=\frac{\hbar^2}{4r_n q m_n^*}\ \text{ and }\ b_p=\frac{\hbar^2}{4r_p q m_p^*} \tag{5}$$

are two fitting parameters that "control" the quantum mechanical effects in the semiconductor, m_n^* and m_p^* denote the effective masses of electrons and holes, and r_n and r_p are dimensionless parameters that account for statistics of electron

 0-7803-7826-1/03/$17.00 © 2003 IEEE

and holes in semiconductor devices. The values of r_n and r_p vary asymptotically from 1, when only the lowest energy subband is occupied (e.g. low temperature), to 3 when the other subbands become populated as well (e.g. high temperature). In our simulations, we have considered $r_n = r_p = 3$, $m_n^* = 0.21 m_0$, and $m_p^* = 0.49 m_0$. Equations (1)-(4) are subject to appropriate boundary conditions and are solved self-consistently for the variables φ, $\sqrt{n}$, $\sqrt{p}$, ϕ_n and ϕ_p. More details related to the numerical implementation of DG model can be found in [10].

II. Analysis of Fluctuations

In this section, the basic idea of our method is described for the computations of fluctuations of threshold voltages in MOSFET devices.

Let A be some parameter of the semiconductor device (e.g. threshold voltage, drain current, etc.) that fluctuate due to random doping fluctuations and/or to random oxide roughness. This parameter can be written as the sum of its average value A_0 and some fluctuations $\tilde{A}$:

$$A = A_0 + \tilde{A}, \quad \left\langle \tilde{A} \right\rangle = 0, \tag{6}$$

where $\left\langle \tilde{A} \right\rangle$ denotes the expected value of $\tilde{A}$. In order to relate the fluctuations of A to the fluctuations of doping at different locations inside the semiconductor device, we discretize the device region in N cells. Then, the doping concentration in the discretization cell i (D_i) can be written as the sum of the average value of the doping at that location (D_{0i}) and some fluctuations $\tilde{D}_i$:

$$D_i = D_{i0} + \tilde{D}_i, \quad \left\langle \tilde{D}_i \right\rangle = 0. \tag{7}$$

An equation similar to (8) can also be written for the fluctuations of oxide thickness:

$$t_j = t_{j0} + \tilde{t}_j, \quad \left\langle \tilde{t}_j \right\rangle = 0, \tag{8}$$

where t_j denotes the corresponding oxide thickness at mesh cell j at the silicon-oxide interface. In the first order approximation, the fluctuations of A can be expressed as a linear combination of the doping and oxide thickness fluctuations:

$$\tilde{A} = \sum_i \frac{\partial A}{\partial D_i} \tilde{D}_i + \sum_j \frac{\partial A}{\partial t_j} \tilde{t}_j = \sum_i \beta_A^i \tilde{D}_i + \sum_j \gamma_A^j \tilde{t}_j, \tag{9}$$

where $\beta_A^i = \partial A / \partial D_i$ and $\gamma_A^j = \partial A / \partial t_j$ are the doping and oxide thickness superposition coefficients of A. These coefficients show how sensitive parameter A is to the fluctuations of doping concentration and oxide thickness at different locations and, therefore, they are very instrumental in the design of dopant fluctuation-resistant structures. Equation (9) allows one to compute σ_A^2 if one knows the statistics of doping concentration and the autocorrelation function (*ACF*) of the oxide thickness fluctuations. If we assume (as it is usually done in literature) that the fluctuations of doping concentration are independent Poisson random variables and they are independent from the fluctuations of oxide thickness, one can evaluate σ_A^2 as follows:

$$\sigma_A^2 = \sum_i \left(\beta_A^i\right)^2 \frac{D_{0i}}{\Delta V_i} + \sum_{j_1, j_2} \gamma_A^{j_1} \gamma_A^{j_2} ACF(j_1, j_2), \tag{10}$$

where (j_1, j_2) are two indices that parameterize the discretized oxide-silicon interface. The *AFC* is defined as:

$$ACF(i,j) = \left\langle \left(t_i - \langle t_i \rangle\right) \cdot \left(t_j - \langle t_i \rangle\right) \right\rangle = \left\langle \tilde{t}_i \cdot \tilde{t}_j \right\rangle. \tag{11}$$

This function can be directly [11] measured but, in most cases, it can be approximated by an exponential distribution function. The problem of the computation of σ_A is thus reduced to the computation of superposition coefficients of parameter A. It can be shown that β_A^i and γ_A^j can be computed numerically with very low computational cost by linearising the transport equations with respect to the fluctuating quantities.

The rest of this section presents the method for the computation of superposition coefficients of the drain current ($A = I_{DS}$) and threshold voltage ($A = V_T$). The method described below is similar to the method presented in [4]. For the sake of brevity, it is convenient to consider the transport equations (7)-(11) in discretized vector form: $\boldsymbol{F}(\boldsymbol{X}, \boldsymbol{D}, \boldsymbol{t}, V_G) = 0$, where $\boldsymbol{X}$ is the state vector (also called variable vector) that consists of the mesh-point values of the potential, electron and hole concentration and quasi-Fermi potentials, $\boldsymbol{D}$ and $\boldsymbol{t}$ are two column vectors whose components are D_i and t_j respectively, V_G is the potential on the gate and $\boldsymbol{F}$ is the "equation" vector that has the same dimension as $\boldsymbol{X}$. If $\tilde{\boldsymbol{X}}$ denotes the fluctuations of the state vector and $\tilde{V}_G$ the fluctuations of the gate potential, than one can write in the first order approximation:

$$\hat{\boldsymbol{F}}_{\boldsymbol{X}} \tilde{\boldsymbol{X}} + \hat{\boldsymbol{F}}_{\boldsymbol{D}} \tilde{\boldsymbol{D}} + \hat{\boldsymbol{F}}_{\boldsymbol{t}} \tilde{\boldsymbol{t}} + \boldsymbol{F}_{V_G} \tilde{V}_G = 0, \tag{12}$$

where $\hat{\boldsymbol{F}}_{\boldsymbol{X}}$, $\hat{\boldsymbol{F}}_{\boldsymbol{D}}$, $\hat{\boldsymbol{F}}_{\boldsymbol{t}}$, and $\boldsymbol{F}_{V_G}$ are the derivatives of $\boldsymbol{F}$ with respect to $\boldsymbol{X}$, $\boldsymbol{D}$, $\boldsymbol{t}$, and V_G, respectively. All these derivatives are computed at the given d.c. bias point and average values for doping concentration and oxide thickness. The drain current can also be written as a function of the state $\boldsymbol{X}$, and $\boldsymbol{D}$:

$$I_{DS} = I(\boldsymbol{X}), \tag{13}$$

At threshold voltage, $\tilde{V}_G = \tilde{V}_T$ and the fluctuations of the drain current are zero because the drain current is constant. Therefore, equation (13) implies:

$$0 = \tilde{I}_{DS} = I_{\boldsymbol{X}} \tilde{\boldsymbol{X}}, \tag{14}$$

where $I_{\boldsymbol{X}}$ is the derivative of I with respect to the state variable. Equations (12) and (14) can be solved for the fluctuations of the gate voltage and one obtains: the following formula for $\tilde{V}_G = \tilde{V}_T$:

0-7803-7826-1/03/$17.00 © 2003 IEEE

$$\tilde{V}_T = -\frac{\boldsymbol{g}^t \cdot \hat{\boldsymbol{F}}_D}{\boldsymbol{g}^t \cdot \boldsymbol{F}_{V_G}} \cdot \tilde{\boldsymbol{D}} - \frac{\boldsymbol{g}^t \cdot \hat{\boldsymbol{F}}_t}{\boldsymbol{g}^t \cdot \boldsymbol{F}_{V_G}} \cdot \tilde{\boldsymbol{t}}\,, \qquad (15)$$

where $\boldsymbol{g}^t$ is the transpose of the column vector $\boldsymbol{g}$ and can be found by solving the following linear system of equations:

$$\hat{\boldsymbol{F}}_X^t \boldsymbol{g} = I_X\,, \qquad (16)$$

where $\hat{\boldsymbol{F}}_X^t$ denotes the transpose of matrix $\hat{\boldsymbol{F}}_X$. By comparing this equation to (9), one observes that the factors that multiply $\tilde{\boldsymbol{D}}$ and $\tilde{\boldsymbol{t}}$ in (19) are the superposition coefficients of threshold voltage.

Concerning the numerical implementation of the method, it is worth observing that most of the matrices and vectors in (16)-(17) are sparse and their elements can be easily computed. For example, most of the components of vector $\boldsymbol{F}_{V_G}$ in (17) are equal to zero because $\boldsymbol{F}$ has only a few equations which are related to V_G (usually these equations are associated with the boundary conditions for system (1)-(4)). The same observation can be made about the elements of matrix $\hat{\boldsymbol{F}}_t$ because the oxide discretization region contains a small number of mesh-points compared to the overall device discretization region. Since at room temperature the doping enters linearly in Poisson equation, the derivatives of $\boldsymbol{F}$ with respect to $\boldsymbol{D}$ (matrix $\hat{\boldsymbol{F}}_D$) can be easily computed analytically, and the numerical implementation is simplified considerably.

III. NUMERICAL RESULTS

The method presented in previous section has been numerically implemented and used to calculate the variances of threshold voltages in MOSFET devices. Throughout the calculations the electron and hole mobilities have been described by the model presented in [12].

The simulations have been performed on a set of MOSFET devices that have a structure similar to the retrograde model presented in [13]. The channel doping concentration decreases from 5×10^{18} cm^{-3} at 20 nm (and deeper) to 5×10^{17} cm^{-3} at the surface according to a truncated Gaussian distribution function. The source and drain dopings have a Gaussian distribution with n-type peak surface concentration of 10^{20} cm^{-3} and vertical struggles of about 8.2 nm that correspond to a junction depth of about 20 nm. The lateral source and drain struggles are about 1.34 nm and the source and drain extensions under the gate are 4 nm. The metallurgical channel length is 40 nm and corresponds to an effective channel length of about 44 nm (the effective channel length has been defined according to [13] by the points where the source-drain doping concentration falls to $2\text{x}10^{19}$ cm^{-3}). The thickness of the oxide is 2 nm and the width of the device is 40 nm. In the presented results, usually one of the above parameters is varied while the other ones are held constant.

First, we have analyzed the threshold voltage fluctuations induced by random doping fluctuations. Figures 1 and 2 present the dependence of σ_{V_T} on the doping concentration and

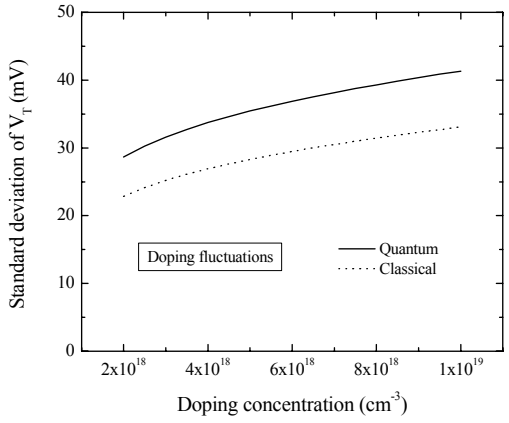

(a)

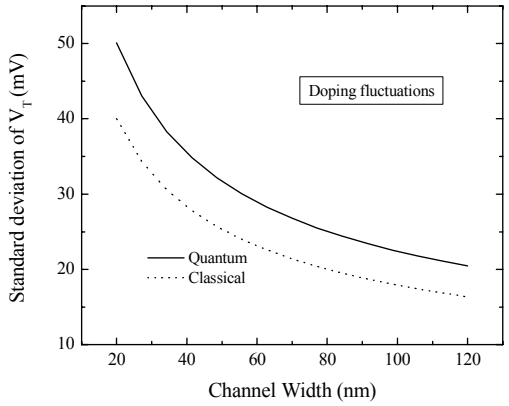

(b)

Figure 1. Standard deviation of V_T as a function of the average doping concentration in the channel (a) and width of the channel(b). Only doping fluctuations are assumed in these simulations.

channel width can be explained qualitatively: the fluctuations of the doping concentration are averaged out by the larger volume of the device and therefore V_T is not as sensitive to these fluctuations. For long devices, it can be proved that $\sigma_{V_T} \sim 1/\sqrt{W}$, where W is the width of the device.

Then, we have investigated the dependence of fluctuations of threshold voltage induced by the random oxide roughness on the doping concentration and channel width. The results of these simulations are presented in Figures 3 and 4, respectively. The autocorrelation function has been assumed to be exponential: $ACF(r) = \Delta^2 \exp(-r/L_c)$, where Δ and L_c are the roughness and the correlation length of the oxide thickness fluctuations. It is worth to observe from these figures that σ_{V_T} increases approximately as $\sqrt{N_a}$ and, for large values of the correlation length, it is practically independent on the oxide channel width. These results are in agreement to those obtained by Asenov et al. [5] by using the Monte-Carlo technique.

0-7803-7826-1/03/$17.00 © 2003 IEEE

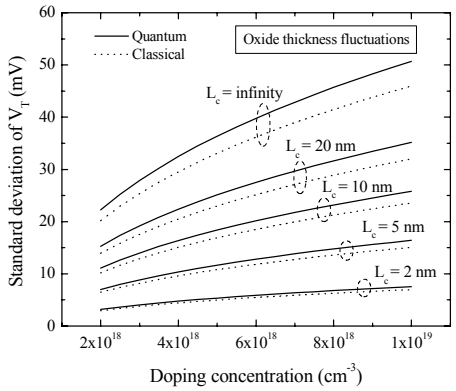

(a)

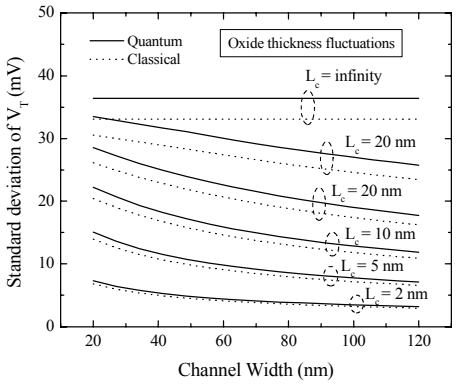

(b)

Figure 2. Standard deviation of V_T as a function of the average doping concentration in the channel (a) and width of the channel (b) for different correlation lengths. Only oxide thickness fluctuations are assumed in these simulations.

Finally, we present the analysis of threshold voltage sensitivity to local fluctuations of the oxide thickness at different points on the semiconductor-oxide interface. This analysis is especially important in the design of fluctuations resistant structures. Figures 8(a) and 8(b) present the classical and quantum (mesh independent) sensitivity coefficients as a function of the (*x, y*) position on the interface. These sensitivity coefficients are defined as $\left(\gamma_{V_T}^{t_j}/\Delta S_j\right)^2$ where ΔS_j is the area of the discretization cell *j* on the surface of the oxide. It can be observed that the threshold voltage is more sensitive to the fluctuations of oxide thickness in the middle region of the oxide layer, but it is quite insensitive to the edge fluctuations of the oxide thickness. This effect and can have positive implications in the fabrication process of the oxide because the ulterior etching and deposition of polysilicon usually deteriorates the edges of the oxide layer.

IV. CONCLUSIONS

A novel technique for the calculations of threshold voltage fluctuations caused by random fluctuations of doping and oxide thickness is presented. This technique circumvents computations for numerous devices and, in addition, it yields the information on sensitivity of threshold voltage fluctuations to local doping and oxide thickness fluctuations. It is demonstrated that the quantum mechanical effects further aggravate the situation by increasing the standard deviations of threshold voltages by 10-15% for 30 nm scale devices.

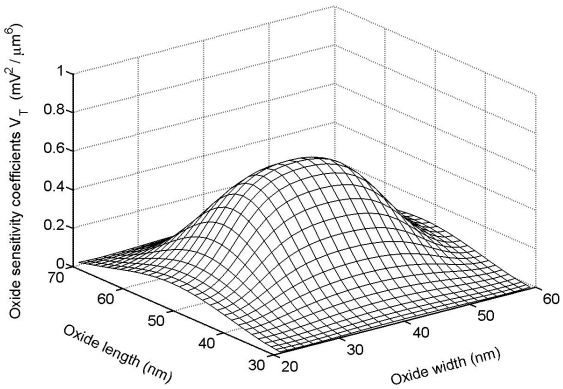

Figure 3. Oxide thickness sensitivity coefficients of threshold voltage.

REFERENCES

[1] H. S. Wong and Y. Taur, "Three dimensional 'atomistic' simulation of discrete random dopant distribution effects in sub-0.1 mm MOSFETs", IEDM Tech. Dig., pp. 705–708, 1993.

[2] I. D. Mayergoyz and P. Andrei, "Statistical analysis of semiconductor devices", J. Appl. Phys. vol. 90, pp. 3019-3029, 2001.

[3] A. Asenov, S. Slavcheva, A. R. Brown, J. H. Davies, and S. Saini, "Increase in the random dopant induced threshold fluctuations and lowering in sub-100 nm MOSFETs due to quantum effect: a 3-D density-gradient simulation study", IEEE Trans. Electron Devices, vol. 48, pp. 722-729, 2001.

[4] I. D. Mayergoyz, P. Andrei, and I. Filipovic, "Analysis of random dopant-induced effects through numerical solution of randomly perturbed nonlinear Poisson equation", IEEE Trans. Magn., vol. 37, pp. 3155-3158,. 2001.

[5] A. Asenov, S. Kaya, and J. H. Davies, "Intrinsic threshold voltage fluctuations in decanano MOSFETs due to local oxide thickness variations", IEEE Trans. Electron Devices, vol. 49, pp. 112-119, 2002.

[6] P. Andrei and I. D. Mayergoyz, "Analysis of random dopant-induced fluctuations of frequency characteristics of semiconductor devices", J. Appl. Phys. vol. 93, pp. 4646-4652, 2003.

[7] I. D. Mayergoyz and P. Andrei, "Numerical analysis of random dopant-induced effects in semiconductor devices", Int. J. High Speed Electronics and Systems, vol. 12, pp. 551-562, 2002.

[8] P. Andrei and I. D. Mayergoyz, "Random doping-induced fluctuations of subthreshold characteristics in MOSFET devices", to appear in Solid-State Electronics, June, 2003.

[9] M. G. Ancona and G. J. Iafrate, "Quantum correction to the equation of state of an electron gas in a semiconductor", Phys. Rev. B, vol. 39, pp. 9536-9540, 1989.

[10] M. G. Ancona, Z. Yu, R. W. Dutton, P. J. V. Voorde, M. Cao, and D. Vook, "Density-gradient analysis of MOS tunneling", IEEE Trans. Electron Devices, vol. 47, pp. 2310-2319, 2000.

[11] T. Yoshinobu, A. Iwamoto, and H. Iwasaki, "Scaling analysis of SiO_2/Si interface roughness by atomic force microscopy", Jpn. J. Appl. Phys., vol. 33, pp. 383-387, 1994.

[12] M. N. Darwish, J. L. Lentz, M. R. Pinto, P. M. Zeitzoff, J. Krutsick, and H. H. Vuong, "An improved electron and hole mobility model for general purpose device simulation ", IEEE Trans. Electron Devices, vol. 44, pp. 1529- 1538, 1997.

[13] Y. Taur, C. H. Wann, and D. J. Frank, "25 nm CMOS design considerations", IEDM 98, pp. 789-792, 1998.

0-7803-7826-1/03/$17.00 © 2003 IEEE